New Phytologist

Research

# Allelic differences of clustered terpene synthases contribute to correlated intraspecific variation of floral and herbivory-induced volatiles in a wild tobacco

**Shuqing Xu[1], Christoph Kreitzer[2], Erica McGale[2], Nathalie D. Lackus[3], Han Guo[2], Tobias G. Köllner[3], Meredith C. Schuman[2,4], Ian T. Baldwin[2] and Wenwu Zhou[5]**

[1]Institute for Evolution and Biodiversity, University of Münster, Hüfferstrasse 1, Münster 48149, Germany; [2]Department of Molecular Ecology, Max Planck Institute for Chemical Ecology, Jena 07745, Germany; [3]Department of Biochemistry, Max Planck Institute for Chemical Ecology, Jena 07745, Germany; [4]Department of Geography & Department of Chemistry, University of Zurich, Zurich 8057, Switzerland; [5]Institute of Insect Sciences, Zhejiang University, Hangzhou 310058, China

Authors for correspondence:
*Shuqing Xu*
*Tel: +49 (0)251 83 21090*
*Email: shuqing.xu@uni-muenster.de*

*Wenwu Zhou*
*Tel: +86 (0)571 88982782*
*Email: wenwuzhou@zju.edu.cn*

Received: *18 February 2020*
Accepted: *29 May 2020*

*New Phytologist* (2020) **228:** 1083–1096
**doi**: 10.1111/nph.16739

**Key words:** allelic variations, *cis*-regulatory elements, ecological pleiotropy, floral volatiles, herbivore-induced plant volatiles, long terminal repeats, QTL mapping, terpene synthase.

## Summary

- Plant volatile emissions can recruit predators of herbivores for indirect defense and attract pollinators to aid in pollination. Although volatiles involved in defense and pollinator attraction are primarily emitted from leaves and flowers, respectively, they will co-evolve if their underlying genetic basis is intrinsically linked, due either to pleiotropy or to genetic linkage. However, direct evidence of co-evolving defense and floral traits is scarce.
- We characterized intraspecific variation of herbivory-induced plant volatiles (HIPVs), the key components of indirect defense against herbivores, and floral volatiles in wild tobacco *Nicotiana attenuata*.
- We found that variation of (*E*)-β-ocimene and (*E*)-α-bergamotene contributed to the correlated changes in HIPVs and floral volatiles among *N. attenuata* natural accessions. Intraspecific variations of (*E*)-β-ocimene and (*E*)-α-bergamotene emissions resulted from allelic variation of two genetically co-localized terpene synthase genes, *NaTPS25* and *NaTPS38*, respectively. Analyzing haplotypes of *NaTPS25* and *NaTPS38* revealed that allelic variations of *NaTPS25* and *NaTPS38* resulted in correlated changes of (*E*)-β-ocimene and (*E*)-α-bergamotene emission in HIPVs and floral volatiles in *N. attenuata*.
- Together, these results provide evidence that pleiotropy and genetic linkage result in correlated changes in defenses and floral signals in natural populations, and the evolution of plant volatiles is probably under diffuse selection.

## Introduction

Plant volatile emissions mediate interactions between plants and their friends and foes at a distance, which significantly affect plant fitness in nature (Dicke, 1994; Baldwin, 2010). When attacked by herbivores, many plants emit herbivory-induced plant volatiles (HIPVs) from their leaves, which attract predators or parasitoids of herbivores, as well as deter herbivore oviposition, thus reducing herbivore loads and increasing the chance of plant survival (Turlings & Wäckers, 2004; Halitschke *et al.*, 2008; Degenhardt *et al.*, 2009; Allmann & Baldwin, 2010; Schuman *et al.*, 2012). For many flowering plants, floral scent is a key signal that attracts pollinators to transfer pollen, and hence is critical for their reproductive success (Raguso, 2008). Interestingly, many of the same volatile organic compounds are found in both floral volatiles and HIPVs, including many terpenoids (Tholl, 2006; Raguso, 2016).

Terpenoids represent the largest class of plant-derived natural products (Boutanaev *et al.*, 2015), and are produced from terpene precursors: isopentenyl diphosphate, geranyl diphosphate or farnesyl diphosphate, by their 'signature enzymes' – terpene synthases (TPSs; Tholl, 2006; Degenhardt *et al.*, 2009). Because terpene precursors are commonly found in different plant tissues and species, changes in terpenoid abundance, in both floral volatiles and HIPVs, are largely determined by the expression and function of TPSs (van Schie *et al.*, 2006; Tholl, 2006; Nagegowda, 2010; Irmisch *et al.*, 2012). Most previous studies have investigated only floral and foliar expression of TPSs and terpenoid emissions in isolation. However, Lee *et al.* (2010) found that a single homoterpene synthase, expressed in both *Arabidopsis* flowers and herbivore-induced leaves, resulted in the biosynthesis of (*E,E*)-4,8,12-trimethyltrideca-1,3,7,11-tetraene in both HIPVs and floral volatiles. Furthermore, recent genomic studies have shown that many TPSs are co-localized in the genome and form different clusters (defined as two or more genes located near to each other in the genome that were evolved from the same common ancestral gene or involved in the same biosynthetic

pathway) (Falara *et al.*, 2011; Chen *et al.*, 2019, 2020), which can result in strong genetic linkages among TPSs that are expressed in different tissues. These studies suggest that pleiotropy or genetic linkage can result in the co-evolution of floral and foliar terpenoid emissions, which may lead to correlated changes in plant–pollinator and plant–herbivore interactions. However, direct evidence of this inference remains scarce.

In *Nicotiana attenuata*, a wild tobacco native to the North American Great Basin Desert, many of the same terpenoids are found in both HIPVs and floral volatiles (Kessler & Baldwin, 2007; Steppuhn *et al.*, 2008; Wu *et al.*, 2008; Gaquerel *et al.*, 2009; Schuman *et al.*, 2009). Analysing the HIPVs in five natural accessions revealed that herbivory-induced (*E*)-β-ocimene and (*E*)-α-bergamotene emissions are variable in *N. attenuata* (Steppuhn *et al.*, 2008; Wu *et al.*, 2008; Schuman *et al.*, 2009). Through manipulation of individual HIPVs in plants, studies showed that (*E*)-α-bergamotene can significantly increase the attraction of predatory bugs to *N. attenuata* (i.e. *Geocoris* spp.) and improve plant fitness under herbivore attack (Kessler & Baldwin, 2001; Halitschke *et al.*, 2008; Schuman *et al.*, 2012). Moreover, increased (*E*)-α-bergamotene emission in leaves by ectopic expression of a maize *TPS* gene in *N. attenuata* also suggested that (*E*)-α-bergamotene may interact with green leaf volatiles to improve plant fitness in populations of emitting or nonemitting plants (Schuman *et al.*, 2015).

Although *N. attenuata* is a predominantly self-fertilizing species, it opportunistically attracts pollinators for outcrossing (Sime & Baldwin, 2003; Kessler *et al.*, 2008; Guo *et al.*, 2019). Analysis of the floral volatiles of *N. attenuata* revealed that both (*E*)-β-ocimene and (*E*)-α-bergamotene are also present (Kessler & Baldwin, 2007). While the emission of (*E*)-α-bergamotene in corolla tubes increases *Manduca sexta* moth-mediated pollination success (Zhou *et al.*, 2017), (*E*)-β-ocimene can elicit distinct electrophysiological responses in the *M. sexta* antennae and may act as a repellent to the moths (Fraser *et al.*, 2003; Kessler & Baldwin, 2007). However, whether the emission of (*E*)-β-ocimene and (*E*)-α-bergamotene in HIPVs and floral volatiles show correlated changes among different genotypes remains unknown.

Here, we first screened the floral volatiles and HIPVs of natural accessions collected from different habits within the range of *N. attenuata*'s geographical distribution. We found that (*E*)-β-ocimene and (*E*)-α-bergamotene in HIPVs and floral volatiles showed correlated changes among *N. attenuata* genotypes. Using both forward and reverse genetic tools, we characterized the genetic mechanisms underlying the variation of (*E*)-β-ocimene and (*E*)-α-bergamotene in HIPVs and floral volatiles, respectively. The results showed that the within-species variation of (*E*)-β-ocimene and (*E*)-α-bergamotene results from expression changes in two clustered *TPS* genes in the TPS-b clade located on chromosome 2: *NaTPS25* and *NaTPS38*, respectively. To further examine whether these two *TPS* genes contributed to the correlated changes of HIPVs and floral volatiles among *N. attenuata* genotypes, we characterized the haplotypes of *NaTPS25* and *NaTPS38* in *N. attenuata* and their associations with HIPV and floral volatiles. The results demonstrated that allelic differences in the *NaTPS25* and *NaTPS38* gene cluster result in correlated changes in both floral volatiles and HIPVs in natural genotypes of *N. attenuata*.

## Materials and Methods

### Plant materials and growth conditions

Seeds of *N. attenuata* Torrey ex. Watson (Solanaceae) natural accessions (genotypes) were collected from a selection of habitats within the range of the species in the southwestern United States (Supporting Information Table S1) and inbred for one generation in the glasshouse in Jena (Germany) except for two inbred lines: Utah and Arizona, which have been self-fertilized for 30 and 22 generations in the glasshouse, respectively. To develop the advanced inter-cross recombinant inbred line (AI-RIL) population, Utah genotype (self-fertilized for 30 generations) and Arizona genotype (self-fertilized for 22 generations) were crossed to generated $F_1$ plants, which were then self-fertilized to generate 150 $F_2$ plants (Zhou *et al.*, 2017). Briefly, in each generation from $F_2$ to $F_6$, we intercrossed *c.* 150 progeny using a random mating and equal contribution crossing design. For generation $F_7$, two seeds from each of the crosses at $F_6$ were germinated and used for the single-seed descendant inbreeding process. In total, five generations of inbreeding were conducted (from $F_6$ to $F_{11}$).

Seeds were germinated following the protocol described by Krügel *et al.* (2002): seeds were sterilized, placed on Gamborg's B5 medium and kept under LD (16 h : 8 h, light : dark) in a growth chamber (Percival, Perry, IA, USA) for 10 d, and then transferred to small TEKU pots for another 10 d in the glasshouse. Subsequently, plants were transferred to 1 liter pots and kept in the glasshouse (26 ± 1°C; 16 h : 8 h, light : dark). For the virus-induced gene silencing (VIGS) experiments, plants in 1 liter pots were transferred to a climate chamber under a constant temperature of 26°C, a 16 h : 8 h (light : dark) light regime and 65% relative humidity (Galis *et al.*, 2013). Watering, fertilization and light regimes were as previously described (Galis *et al.*, 2013; Schuman *et al.*, 2014).

### Measuring leaf volatiles among 25 natural genotypes and AI-RILs

To measure the emission of leaf volatiles from the 25 natural genotypes, plants in the elongation stage (50 d after germination) were used. Simulated herbivory treatments and leaf volatile collection were conducted as described in detail in a previous study (Zhou *et al.*, 2017). Briefly, the simulated herbivory treatment was carried out at 08:00 h, the leaves were wounded with a pattern wheel, and 20 µl diluted (1 : 5 dilution with water) *M. sexta* oral secretion was supplied to the wounds. To obtain temporally resolved comparative data for leaf volatiles, small pieces of polydimethylsiloxane tubes (see Kallenbach *et al.*, 2014) were incubated with the damaged leaves from 12:00–16:00 h, 16:00–20:00 h and 20:00–06:00 h (the following morning). To measure the effects of jasmonic acid signaling on the induction of leaf volatiles in the 25 genotypes, plants in the elongation stage (55 d after germination) were treated with methyl jasmonate (MeJA).

At 08:00 h, 150 μg MeJA dissolved in 40 μl lanolin paste was deposited at the base of one stem leaf of each plant. After 24 h of the MeJA treatment, the leaf was enclosed in a plastic cup (polyethylene terephthalate) together with two polydimethylsiloxane tubes, and the polydimethylsiloxane tubes were collected 24 h later and kept at −20°C until analysis. Three biological plant replicates were sampled for each group.

The measurement of leaf volatiles from the AI-RIL plants (55 d after germination) has been previously described (Zhou *et al.*, 2017). Briefly, simulated herbivory treatment was carried out at 08:00 h, and the leaf was immediately enclosed in a plastic cup where two polydimethylsiloxane tubes were incubated as described above. The polydimethylsiloxane tubes were collected after 24 h (08:00 h the next day), and immediately kept at −20°C until analysis.

## QTL mapping

To identify the genetic basis underlying HIPV variations in *N. attenuata*, we used a forward genetic mapping approach. The quantitative trait locus (QTL) mapping was described in detail in our previous study (Zhou *et al.*, 2017) and was conducted with the R package QTLREL (Cheng *et al.*, 2011) following the tutorial. In brief, the genotype information of AI-RIL plants and the linkage map were obtained from a dataset reported earlier (Zhou *et al.*, 2017; Guo *et al.*, 2020). In total, we obtained 25 469 single nucleotide polymorphism (SNP) markers among 248 individuals. These markers were grouped into 12 linkage groups. The peak area of herbivore-induced (*E*)-β-ocimene was log-transformed. Samples with missing genotype or phenotype information were removed. The variance of (*E*)-β-ocimene within the population was estimated via 'estVC', and then used for the genome-wide scan together with the genotypes. The empirical threshold was estimated based on 500 permutations.

## Sequencing and assembling the leaf transcriptome of the Arizona genotype

To identify candidate genes that are associated with (*E*)-β-ocimene biosynthesis, we sequenced the transcriptomes of both control and *M. sexta* oral secretion-induced rosette leaves using the Illumina HiSeq 2000 system (San Diego, CA, USA). The growth conditions and simulated herbivory treatments were as described above. Samples from untreated plants were used as control. All samples were collected at 12:00 h. Total RNA was extracted from *c.* 100 mg of plant tissue using TRIzol (Thermo Fisher Scientific, Waltham, MA, USA) according to the manufacturer's protocol. All RNA samples were subsequently treated with DNase-I (Fermentas, Burlington, ON, Canada) to remove all genomic DNA contamination. The mRNA was enriched using an mRNA-seq sample preparation kit (Illumina), and *c.* 200 bp insertion size libraries were constructed using the Illumina whole transcriptome analysis kit following the manufacturer's standard protocol (HiSeq system; Illumina). All libraries were then sequenced on the Illumina HiSeq 2000 at the sequencing core facility at Max Planck Institute for Molecular Genetics (Berlin, Germany). After removing the adaptor sequences and low-quality reads, in total we obtained 25 297 814 and 19 124 690 paired-end 100 bp reads for control and induced samples, respectively. The raw reads have been deposited in the NCBI SRA repository (SRX1804553 and SRX1804540).

The RNA-seq reads from control and induced samples were pooled for *de novo* assembly of the leaf transcriptome from the Arizona genotype using the TRINITY tool kit (Grabherr *et al.*, 2011). The minimum contig length was set at 200 bp. In total, we assembled 62 132 transcripts with N50 length equal to 1364 bp.

## Measuring abundance of *NaTPS25* transcripts in natural accessions

To measure the abundance of *NaTPS25* transcripts in the 25 natural accessions, plants in the elongation stage (50 d after germination) were used. Simulated herbivory treatment was carried out on one stem leaf of each plant at 08:00 h. Eight hours after treatment, the leaf was harvested and immediately kept at −80°C until use. Total RNA was isolated from the leaves using TRIzol reagent (Thermo Fisher Scientific) and then treated with DNase-I (Fermentas) following the manufacturers' instructions, to remove contamination from genomic DNA. One microgram of total RNA from each sample was reverse transcribed into cDNA using SuperScript II reverse transcriptase following the manufacturer's instructions (Thermo Fisher Scientific). The relative transcript accumulation of *NaTPS25* was measured using reverse transcriptase PCR (RT-PCR) on a Stratagene MX3005P PCR cycler (Stratagene, La Jolla, CA, USA). The elongation factor-1A gene, $NaEF_1a$ (accession number D63396), was used as the internal standard for normalization (Oh *et al.*, 2013). PCR amplification was performed with Phusion Green High-Fidelity DNA polymerase (Thermo Fisher Scientific) using 40 PCR cycles to enable the detection of rare transcripts of *NaTPS25*. The primers used are given in Table S2.

## Silencing *NaTPS25* using VIGS, and measurement of HIPVs from VIGS plants

To investigate the function of *NaTPS25 in vivo*, VIGS based on the tobacco rattle virus was used to transiently knock down expression of the *NaTPS25* gene in *N. attenuata* as previously described (Galis *et al.*, 2013). A 163 bp fragment of the open reading frame region of *NaTPS25* was amplified by PCR with the primers listed in Table S2. PCR fragments were separated by agarose gel electrophoresis, excised and purified by a gel band purification kit (Amersham Biosciences, Little Chalfont, UK) according to the manufacturer's instructions. Subsequently, they were digested with *Bam*H1 and *Sal*1 and inserted into plasmid pTV00. After sequencing, the VIGS constructs and pTV00 (empty vector, EV) were separately transformed into *Agrobacterium*. Additionally, the pTVPDS vector, harboring a part of the sequence of a phytoene desaturase, was used to monitor progress of the gene silencing.

The VIGS experiments were carried out on the Arizona genotype. Inoculation was performed 25 d after germination, and

volatile trapping another 20 d later, after establishment of the viral vector. Before any treatment, three leaves (one per plant) were sampled to test silencing efficiency. Afterwards another three leaves (one per plant) were treated with 75 μg MeJA dissolved in 20 μl lanolin paste on the base of leaves at 12:00 h. After 1 h, the outer portion of these leaves was harvested and frozen to test the silencing efficiency, after which the whole plant was again trapped for volatile collection. Lanolin paste (20 μl) was used for the control group.

### Cloning and heterologous expression of NaTPS25

To examine the enzymatic function of *NaTPS25 in vitro*, a truncated version of *NaTPS25_AZ* (missing the first 13 codons) was cloned from cDNA of Arizona genotype plants using the primer pair TPS25f/r (Table S2). The resulting PCR fragment was cloned into the pET200/D-TOPO vector (Invitrogen) and the *Escherichia coli* strain BL21 Codon Plus (Invitrogen) was used for heterologous expression. The protein expression and bacterial extract preparation were done as described in a previous study (Zhou *et al.*, 2017). Enzyme assays were performed in a Teflon-sealed, screw-capped 1 ml GC glass vial containing 50 μl of the bacterial extract and 50 μl assay buffer with 10 μM geranyl diphosphate, 10 mM $MgCl_2$, 0.2 mM $Na_2WO_4$ and 0.1 mM NaF. A solid phase micro-extraction (SPME) fiber coated with a 100 μm thick layer of polydimethylsiloxane (Supelco, Belafonte, PA, USA) was placed into the headspace of the vial where it was incubated for 60 min at 30°C, before it was inserted into the injector of the gas chromatograph to analyze the absorbed reaction products. GC-MS analysis was conducted using an Agilent 6890 Series gas chromatograph coupled to an Agilent 5973 quadrupole mass-selective detector. The gas chromatograph was operated with a DB-5MS column (30 m × 0.25 mm × 0.25 μm; Agilent, Santa Clara, CA, USA).

### Targeted resequencing of the cDNA and genomic regions of *NaTPS38* and confirmation of the inversion of *NaTPS25* in Utah genotype

To sequence the *NaTPS38* locus from all the accessions and characterize its allelic variations, we amplified the full-length open reading frame using high-fidelity Phusion DNA Polymerase (Thermo Fisher Scientific) and the primer combination TPS38f and TPS38r (Table S1). The following cycle parameters were used: 98°C for 30 s; 35 cycles of 98°C for 10 s, 52°C for 20 s and 72°C for 1.5 min; and a final step of 72°C for 5 min. PCR products were separated by agarose gel electrophoresis, excised and purified with a PCR clean-up gel extraction kit (Macherey-Nagel, Düren, Germany), then cloned into the pJET 1.2/blunt vector (Thermo Fisher Scientific) and transformed into *E. coli* (TOP10 Competent Cells; Invitrogen) according to the manufacturers' instructions. Plasmid extraction was performed using the NucleoSpin Plasmid Kit (Macherey-Nagel). Sequencing reactions were performed using the BigDye Terminator mix (Thermo Fisher Scientific). The obtained sequences were manually corrected, and data analysis was executed with GENEIOUS 6.0.5. The cDNA sequences have been deposited in the GenBank Nucleotide Sequence Database (accession nos. MN400683–MN400708).

To examine the genetic architecture of *NaTPS25*, we isolated genomic DNA from 10-d-old seedlings using a cetrimonium bromide (CTAB) extraction buffer (Bubner *et al.*, 2004). Genomic DNA purity and integrity were evaluated by amplifying the elongation factor-1A with the primer set shown in Table S2. Sequencing approaches for the comparison between Arizona genotype and traced fragments in Utah genotype were conducted as described above. PCR fragment amplifications were carried out using Phusion Green DNA Polymerase (Thermo Fisher Scientific) in 20 μl PCRs (×1 Phusion Green HF Buffer, 10 mM dNTPs, 3% DMSO and 5 mM primers). The PCR program (30 s at 98°C, 35 cycles of 10 s at 98°C, 30 s at 60°C and 2 min at 72°C, with a final elongation of 5 min at 72°C) varied in annealing temperature (72°C) according to the primer set (Table S2). We validated the presence of the intact *NaTPS25* allele with primer set I (PrS I), and the presence of exon 6–7 with PrS II. Moreover, we utilized two primer combinations to provide genetic information for the inversion event of exons 6 and 7. PrS II was used to detect exons 6 and 7, and primer PrS III to amplify a fragment specific to this inversion.

### Measuring the abundance of *NaTPS38* transcripts in hybrid plants

To characterize whether the variations of transcript abundance of *NaTPS38* were due to changes in *cis*- or *trans*-regulatory elements, we measured the abundance of *NaTPS38* transcripts in the two parental inbred lines and their hybrid lines in $F_1$. Plants in their elongation stage (50 d after germination) were used. Simulated herbivory treatment was carried out at 08:00 h on one stem leaf of each plant. Eight hours after treatment, leaves were harvested and flash-frozen in liquid nitrogen, then kept at −80°C until processing. Total RNA isolation, cDNA synthesis and quantitative PCR (qPCR) amplification were carried out as described above. The primers used to specifically amplify the alleles are shown in the Supporting Information (Table S2).

### Statistical analysis

All statistical analyses were performed in R 3.5.1 (R Core Team, 2016). The functions 'prcomp', 't.test' and 'anova' from the STATS package were used for principal components analysis, Student's *t*-tests and ANOVA analysis, respectively. The raw data and data analysis R scripts are deposited in the figshare repository: https://doi.org/10.6084/m9.figshare.11848137.v1.

## Results

### (*E*)-β-ocimene and (*E*)-α-bergamotene contributed to associated changes in HIPVs and floral volatiles among *N. attenuata* natural accessions

We first investigated HIPV variations in *N. attenuata* by sampling the herbivory-induced leaf headspace from 25 genotypes that were

collected from different habitats within the species range. We found two monoterpenes, (*E*)-β-ocimene and linalool, and one sesquiterpene, (*E*)-α-bergamotene, to be highly variably released among the studied genotypes (Fig. 1a–c). In addition, previous studies have shown that the emission of all three compounds in leaves was significantly induced by herbivory (Halitschke *et al.*, 2000), supporting their classification as HIPVs. Jasmonate signaling is involved in regulating the emission of many HIPVs in *N. attenuata*, and its accumulation is variable among wild genotypes (Schuman *et al.*, 2009). To examine whether the observed HIPV variations were attributable to differences in herbivory-induced jasmonate signaling, we supplied a similar level of MeJA to the leaves of these genotypes. Under similarly elevated levels of jasmonate signaling in MeJA-treated plants, the emission of the three terpenoids remained variable and were the major contributors to the variation in HIPVs among the investigated genotypes (Fig. 1d). This suggests that intraspecific variations of HIPVs are largely independent of jasmonate signaling.

In addition to a flower-specific volatile, benzoyl acetone (Guo *et al.*, 2020), the three terpenoids in HIPVs, (*E*)-β-ocimene, linalool and (*E*)-α-bergamotene, were also found in *N. attenuata* floral volatiles (Kessler & Baldwin, 2007). We reasoned that if the same compound in HIPVs and floral volatiles was regulated by the same genetic mechanism, its abundance would show correlated changes in amounts of HIPVs and floral volatiles among different genotypes. To examine this, we further measured the floral volatiles of the 25 genotypes and compared the emissions of (*E*)-β-ocimene, linalool and (*E*)-α-bergamotene emission in the HIPVs and floral volatiles. We found that linalool, which was found in both floral volatiles and HIPVs, showed no correlation among the different genotypes, consistent with a recent study (He *et al.*, 2019). However, the variations of (*E*)-α-bergamotene and (*E*)-β-ocimene emission in HIPVs and floral volatiles were significantly correlated (Fig. 1; (*E*)-β-ocimene: $R^2 = 0.23$, $P = 0.021$; (*E*)-α-bergamotene: $R^2 = 0.50$, $P < 0.001$).

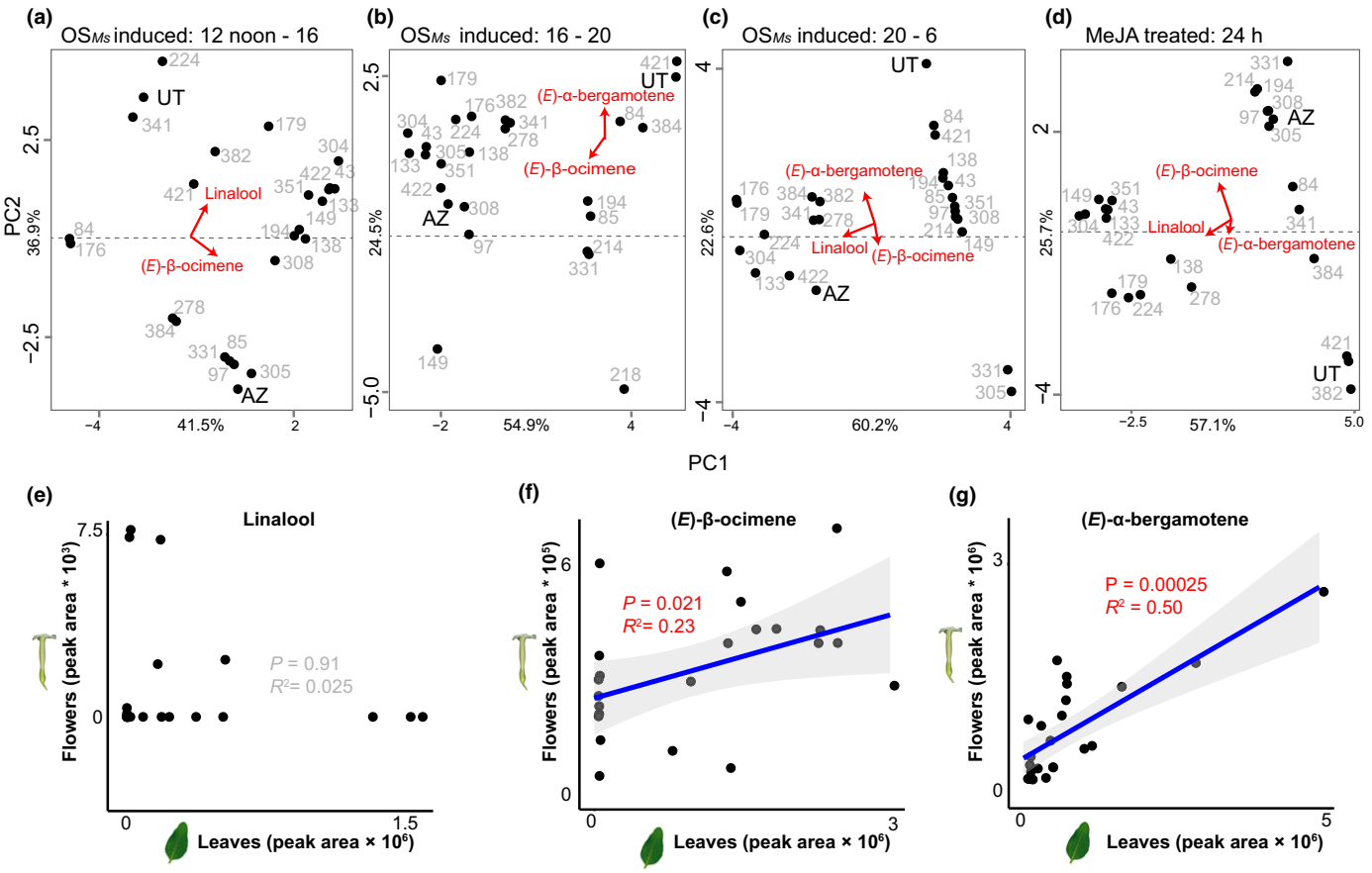


**Fig. 1** Variations of herbivory-induced plant volatiles (HIPVs) and correlated changes between HIPVs and floral volatiles. (a–d) Principal component analysis of leaf volatiles after simulated herbivory (a–c), or after MeJA treatment (d). For simulated herbivory treatment ($OS_{MS}$), leaves were treated with wounding and oral secretion of *Manduca sexta* at 08:00 h, and headspace compositions were sampled over three different time periods (12:00–16:00 h, 16:00–20:00 h and 20:00 h–06:00 h) after the OS induction. For MeJA treatment, volatiles were sampled from leaves in a single incubation, 24–48 h after treatment. Variance explained by PC1 and PC2 is shown on the *x*-axis and *y*-axis, respectively. The four plots should not be compared among each other because the variance/covariance structure of the data is not the same. (e–g) Correlated emission changes between flowers and MeJA-treated leaf headspaces among different genotypes were found in (*E*)-α-bergamotene and (*E*)-β-ocimene but not linalool. Each dot represents a genotype. Spearman rank correlations were used for estimating *P*-values and $R^2$. Ribbons indicate 95% confidence intervals.

### Changes in *NaTPS25* and *NaTPS38* expression are associated with intraspecific variations of (*E*)-β-ocimene and (*E*)-α-bergamotene emissions, respectively, in both HIPVs and floral volatiles

To characterize the genetic mechanisms underlying the correlated changes of (*E*)-α-bergamotene and (*E*)-β-ocimene emission in HIPVs and floral volatiles, we used both forward and reverse genetic tools.

We have previously established an AI-RIL population that was derived from crossing the Arizona and Utah genotypes whose (*E*)-β-ocimene and (*E*)-α-bergamotene emissions differed in HIPVs and floral volatiles. Using this population, we identified a terpene synthase, *NaTPS38*, on linkage group 2 that controls the emissions of (*E*)-α-bergamotene in both HIPVs and floral volatiles (Zhou *et al.*, 2017). Among different *N. attenuata* genotypes, the changes in *NaTPS38* expression were correlated with (*E*)-α-bergamotene emissions in both HIPVs and floral volatiles (Zhou *et al.*, 2017).

Here, using a similar approach, we found that variations in (*E*)-β-ocimene emission in HIPVs were mapped to the same locus as *NaTPS38* on linkage group 2 of *N. attenuata* (Fig. 2a; Zhou *et al.*, 2017). This location overlaps with a terpene synthase cluster, which contains a subclade of TPS-b monoterpene synthase genes, including *TPS25*, *TPS27* and *TPS38* (Falara *et al.*, 2011). Among these genes, *TPS25* and *TPS27* in tomato were highly similar to the grape *VvTPS47* that produces (*E*)-β-ocimene. However, after searching the draft genome of *N. attenuata* (created using the Utah genotype), we did not find any genes that showed high similarity to either *TPS25* or *TPS27*. Sequencing the transcriptome of the Arizona genotype allowed us to identify *NaTPS25*, which showed high similarity to *TPS25* and *TPS27* in tomato.

To examine the enzymatic function of *NaTPS25*, we measured the TPS activity of *NaTPS25 in vitro* by heterologous expression of the gene in *E. coli*. The recombinant NaTPS25 protein converts the substrate geranyl diphosphate into (*E*)-β-ocimene as its only product (Fig. 2b). To examine the function of *NaTPS25 in vivo*, we silenced the expression of *NaTPS25* in *N. attenuata* (Arizona genotype) using VIGS. When *NaTPS25* expression was silenced, levels of both constitutive and MeJA-induced (*E*)-β-ocimene emission in HIPVs were strongly reduced (Fig. 2c,d). Together, these results suggest that herbivore-induced (*E*)-β-ocimene is associated with the expression of *NaTPS25* in HIPVs.

We further investigated whether the expression changes in *NaTPS25* are associated with (*E*)-β-ocimene in HIPVs and floral volatiles. We first measured the presence of *NaTPS25* transcripts among the 25 genotypes by RT-PCR. Interestingly, we observed presence and absence variations of *NaTPS25* at the level of transcripts, which correlate with the emission of (*E*)-β-ocimene from induced leaves among genotypes (Fig. 3a). While *NaTPS25* transcripts can be found in all 15 genotypes that emitted (*E*)-β-ocimene after simulated herbivory, they were not found in any of the other 10 genotypes that did not emit detectable levels of (*E*)-

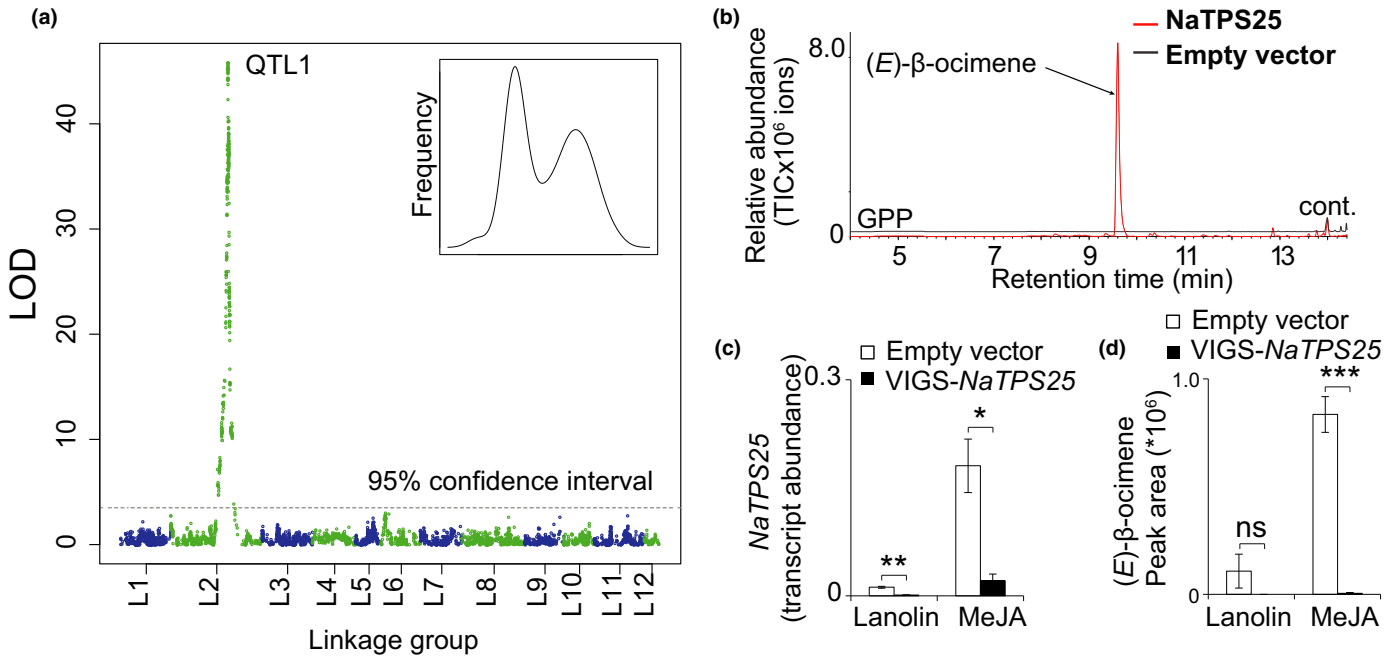


**Fig. 2** QTL mapping for (*E*)-β-ocimene and functional validation of *NaTPS25*. (a) One QTL locus on linkage group 1 (QTL1) for (*E*)-β-ocimene. The 95% confidence interval is marked with a dashed line. (b) Heterologously expressed NaTPS25 protein produces (*E*)-β-ocimene *in vitro*. Total ion chromatograms (GC-MS) of the empty vector control (black solid line) and the enzyme products of NaTPS25 protein (red solid line).The enzyme was expressed in *Escherichia coli* and incubated with the substrate geranyl diphosphate. (c, d) Virus-induced gene silencing (VIGS)-mediated silencing of *NaTPS25* expression in leaves. Both constitutive (lanolin) and MeJA-induced levels of *NaTPS25* transcript abundance (c) and (*E*)-β-ocimene emission (d) were measured ($n = 4$). Mean and SE are shown. ns, not significant; TIC, total ion count . Statistical differences are determined by Student's *t*-test. *, $P < 0.05$; **, $P < 0.01$; ***, $P < 0.001$.

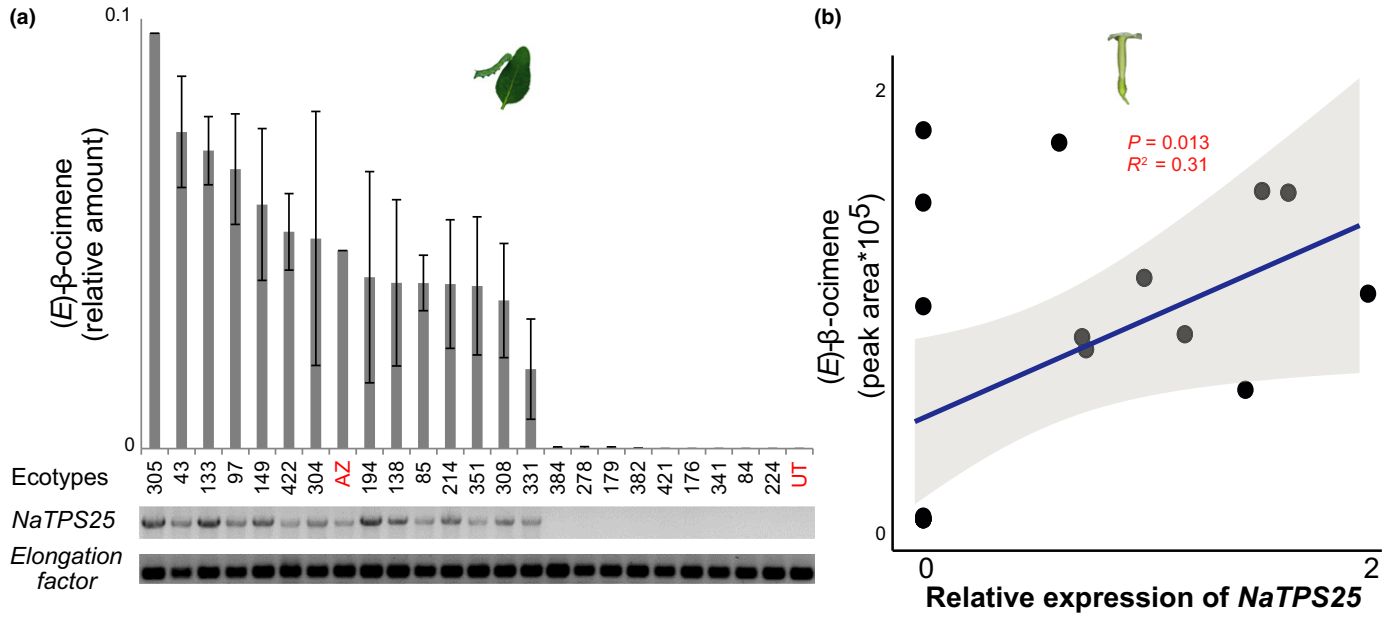


**Fig. 3** Correlation between transcript abundance and (*E*)-β-ocimene emission. (a) Expression of *NaTPS25* and (*E*)-β-ocimene emission in herbivory-induced leaves. *x*-axis: the names of accessions and the RT-PCR result of *NaTPS25* and *elongation factor-1A* (housekeeping gene); *y*-axis: the relative amount of (*E*)-β-ocimene in the herbivory-induced plant volatiles (HIPVs) (normalized to all compounds). The leaves were wounded and treated with oral secretion of *Manduca sexta* larvae at 08:00 h, volatiles were collected from 12:00–16:00 h ($n = 3$) and leaf samples for expression analysis (RT-PCR for *NaTPS25*) were collected at 16:00 h on the same day ($n = 3$). Mean and SE are shown. (b) Expression of *NaTPS25* and (*E*)-β-ocimene emission in flowers. Spearman rank correlations were used for estimating *P*-values and $R^2$. Ribbons indicate 95% confidence intervals.

β-ocimene (Fig. 3a). We then used qPCR to measure the transcript abundance of *NaTPS25* in flowers in order to compare them to emissions of (*E*)-β-ocimene in the respective floral volatile profiles of each genotype. We found that among different genotypes, emissions of (*E*)-β-ocimene in floral volatiles were significantly correlated with *NaTPS25* transcript abundance ($P = 0.013$, Fig. 3b). Interestingly, while most of the genotypes that had a high abundance of *NaTPS25* transcripts also had a high floral (*E*)-β-ocimene emission, a few genotypes (e.g. genotype Utah, 43 and 351) showed very low levels of *NaTPS25* transcript abundance, yet still emitted high levels of (*E*)-β-ocimene in their flowers (Fig. 3b). These results suggest that in addition to *NaTPS25*, other genes are involved in floral (*E*)-β-ocimene emission. Consistently, in the *N. attenuata* genome (Utah genotype), there is another member of the TPS-b subfamily, of which several homologs from *Vitis vinifera* and *Arabidopsis thaliana* can synthesize (*E*)-β-ocimene *in vitro* using geranyl diphosphate as the substrate (Huang *et al.*, 2010; Martin *et al.*, 2010). Furthermore, one homolog of *TPS19* (NIATv7_g29416), which is a member of TPS-e/f subfamily that can produce (*E*)-β-ocimene using neryl pyrophosphate substrate (Matsuba *et al.*, 2013), was found highly to be expressed in the flowers of *N. attenuata* (http://nadh.ice.mpg.de/NaDH-eFP/cgi-bin/efpWeb.cgi; Brockmöller *et al.*, 2017).

Together with our previous study (Zhou *et al.*, 2017), these results suggest that expression changes in *NaTPS25* and *NaTPS38* are associated with intraspecific variations of (*E*)-β-ocimene and (*E*)-α-bergamotene emissions, respectively, in HIPVs and floral volatiles.

## Two distinct genetic mechanisms resulted in changes in allelic expression of *NaTPS25* and *NaTPS38*

To investigate the genetic mechanisms underlying the allelic expression differences in *NaTPS25* and *NaTPS38*, we analyzed sequence polymorphisms of *NaTPS25* and *NaTPS38* among different genotypes.

Consistent with its presence and absence of detectable transcripts levels, we found a structural variation in the *NaTPS25* gene among different genotypes. For genotypes that emit (*E*)-β-ocimene and express *NaTPS25* after simulated herbivory or MeJA treatment, the complete *NaTPS25* gene can be amplified from genomic DNA with primers that bind to regions containing the start codon and stop codon (Fig. 4a,b). There was no obvious gene size variation among these genotypes (Fig. 4b). However, for the accessions that failed to emit (*E*)-β-ocimene, *NaTPS25* cannot be amplified using the same primers. Designing exon-specific primers and comparing the genomic sequences of *NaTPS25* revealed that the Utah genotype contains two fragments of *NaTPS25*, disrupted by a *c.* 9 kb long terminal repeat (LTR)-gypsy transposon. The first fragment contains only exons 6 and 7, whereas the second fragment contains partial sequences of exons 2 and 7 (Fig. 4a). Using two primer pairs that can specifically amplify these two fragments among different genotypes, we found that most of the genotypes that failed to emit (*E*)-β-ocimene after simulated herbivory shared the same disrupted gene structure (Fig. 4c). Furthermore, additional genomic changes to the *NaTPS25* fragments were found in some genotypes, such as genotype 421, in which the joined fragments

New Phytologist

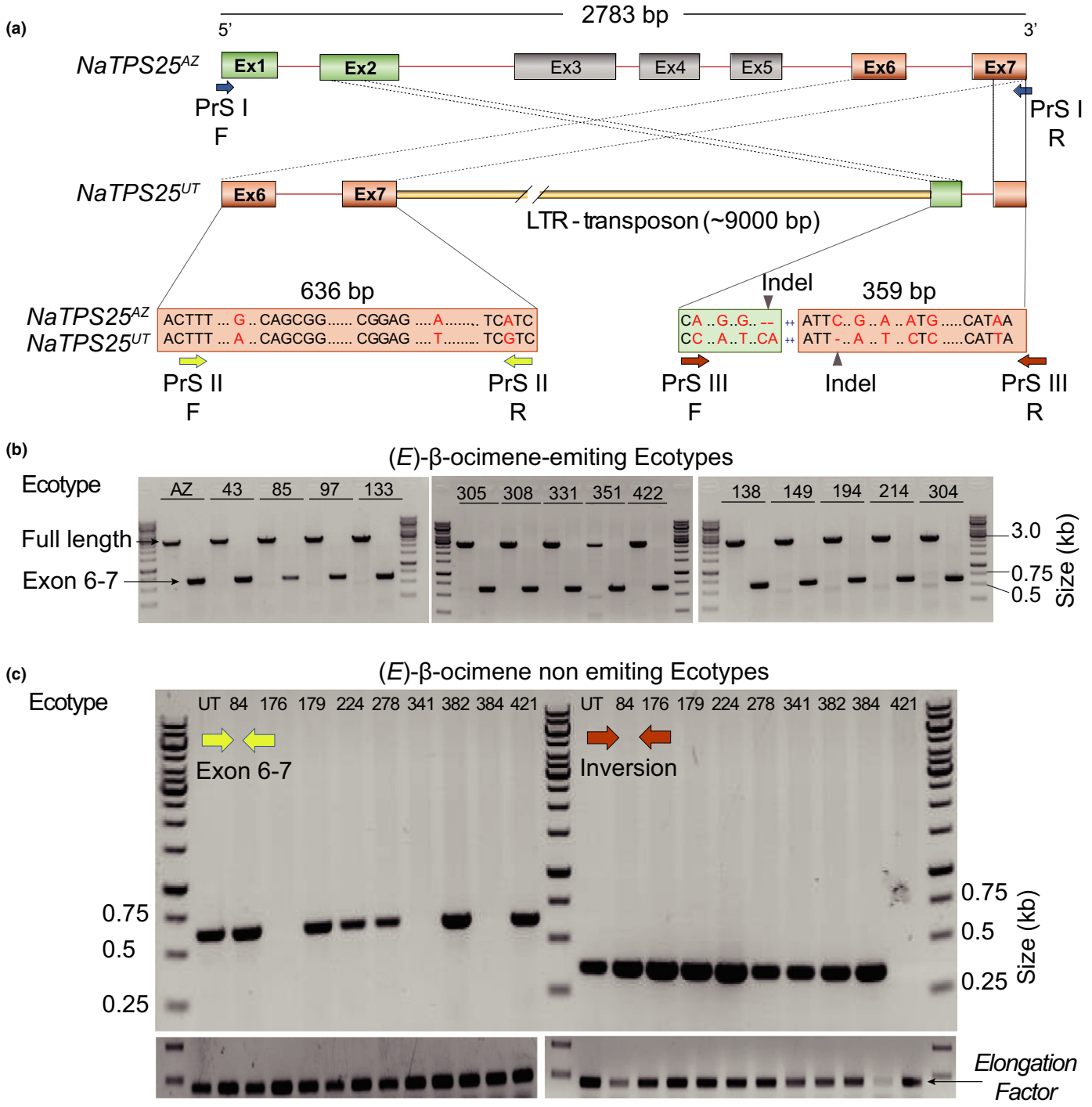


**Fig. 4** Allelic variation of *NaTPS25* among *Nicotiana attenuata* natural accessions. (a) The structure of the complete and the inverted *NaTPS25* alleles in *N. attenuata*. The active *NaTPS25* allele in the Arizona genotype consists of seven exons (rectangles, Ex1-7) and six introns (red lines). A disruption in the *NaTPS25* allele of the Utah genotype was found by an insertion of a *c*. 9 kb LTR-gypsy transposon (discontinuous yellow rectangle). Dashed lines illustrate partially inverted fragments in the Utah genotype, in comparison to the allele in the Arizona genotype. Alignment of detected fragments in Utah and Arizona genotypes suggested four SNPs (red letters). Two descended regions of the active allele (parts of exons 2 and 7) are linked with a region whose origin is unclear and forms the second fragment (green and orange boxes). Dots refer to the consensus sequences. (b) The full-length *NaTPS25* PCR fragment was amplified in (*E*)-β-ocimene-emitting genotypes (HIPVs). Primerset (PrS) I (blue arrows) and PrS II (yellow green arrows) from (a) were used to amplify the full-length and exons 6 and 7, respectively. (c) Presence/absence of exons 6 and 7 and the inversion region among non-(*E*)-β-ocimene-emitting genotypes (HIPVs). Fragments of exons 6 and 7 and the inversion region were amplified with PrS II (yellow green arrows) and PrS III (brown arrows).

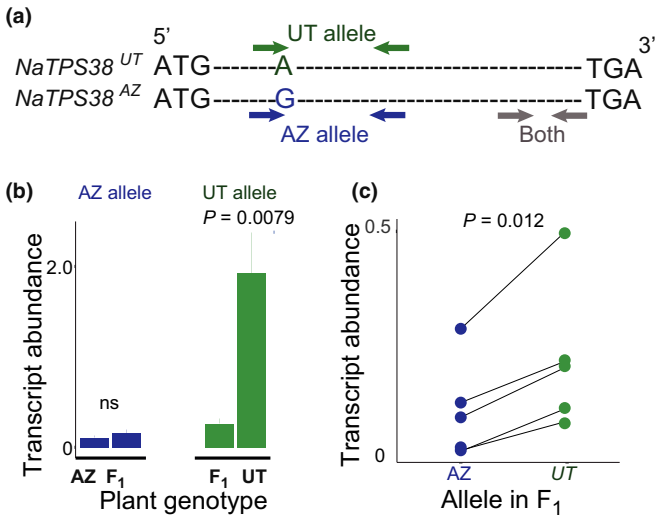


**Fig. 5** Allelic expression of *NaTPS38* in $F_1$ hybrids of Arizona and Utah genotypes. (a) Scheme of primers used to measure the allele-specific transcript abundance. Green arrows refer to primers that can specifically amplify the Utah allele and blue arrows refer to primers that can specifically amplify the Arizona allele. Primers (gray arrows) that do not distinguish the two alleles were also used to measure total transcript abundance of *NaTPS38*. (b) Expression differences of *NaTPS38* alleles between $F_0$ and $F_1$ plants. Plants were treated with wounding plus oral secretion ($n = 5$). Mean and SE are shown. Student's *t*-test was used to determine differences between $F_0$ and $F_1$ plants. ns, no significant difference was found. (c) Expression differences of alleles in $F_1$ individuals. Plants were treated with wounding plus oral secretion ($n = 5$). Each dot represents an individual plant. Difference between two alleles was determined by a paired Student's *t*-test. Blue and green colors indicate alleles from Arizona and Utah genotypes, respectively.

between exon 2 and exon 7 could not be amplified, and genotypes 176, 341 and 384, in which the exon 6 and 7 fragments could not be amplified. These results showed that allelic differences of *NaTPS25*, caused by LTR-gypsy transposon insertions, contributed to the variations of (*E*)-β-ocimene emission in the HIPVs among different genotypes.

*NaTPS38* transcripts were found in all genotypes but differed in their abundances (Zhou *et al.*, 2017). To test whether polymorphic sites at a *cis*-regulatory region and/or changes in *trans*-regulatory elements contributed to the observed variations in the expression of *NaTPS38*, we measured the abundance of *NaTPS38* transcripts in the plants from Arizona and Utah genotypes and their $F_1$ progeny. Because all the *trans* factors are shared amongst the $F_1$ progeny, differences in allelic transcript abundance between parents and $F_1$ indicate changes in relative *trans*-regulatory activity, whereas differences in relative transcript abundance between two alleles in $F_1$ indicate changes in relative *cis*-regulatory activity (Wittkopp, 2013). After simulated herbivore elicitation, while transcript levels of the *NaTPS38* Arizona allele did not differ between parental and $F_1$ plants (Fig. 5, $P > 0.1$), levels of the *NaTPS38* Utah allele were significantly lower in $F_1$ plants than in the Utah genotype ($P = 0.0079$, Student's *t*-test), suggesting that the Arizona genotype carries a *trans*-suppressor of *NaTPS38*. In addition, the relative transcript abundances of Arizona and Utah alleles in $F_1$ plants were significantly different (Fig. 5, paired Student's *t*-test, $P = 0.012$), indicating that the *cis*-regulatory activity of *NaTPS38* is different between Arizona and Utah genotypes. We further sequenced the upstream regulatory region of *NaTPS38* in both Arizona and Utah genotypes. In comparison to the Utah genotype, the Arizona genotype has a 129 bp insertion and one SNP (change from A to G) within the 1 kb upstream region of *NaTPS38* (Fig. S1). In summary, polymorphisms at both *trans*- and *cis*-regulatory regions contribute to allelic differences of herbivory-induced *NaTPS38* expression and therefore (*E*)-α-bergamotene emission in *N. attenuata*.

## Allelic variations of *NaTPS25* and *NaTPS38* resulted in correlated changes of (*E*)-β-ocimene and (*E*)-α-bergamotene emission in HIPVs and floral volatiles in *N. attenuata*

We further explored whether the correlated changes in (*E*)-β-ocimene and (*E*)-α-bergamotene emission in HIPVs and floral volatiles are due to allelic variations of *NaTPS25* and *NaTPS38*. To this end, we first sequenced the full-length open reading frame of *NaTPS38* from the 25 natural genotypes. None of these contained either a premature stop codon or an insertion/deletion (Fig. 6a). The *NaTPS38* transcripts could be classified into three different haplotypes (YGI, HGV and YEI) that resulted from three common polymorphic nonsynonymous substitution sites: Y32H, G280E and I450V. Mapping these amino acid changes to the protein model of NaTPS38 suggested that Y32H and G280E are not involved in the formation of the active site cavity, although I450V is part of a loop structure near the entrance of the active site cavity (Fig. S2). However, the substitution I450V was found both in genotypes that emit high (e.g. genotype 304) and low levels (e.g. genotype 85) of herbivory-induced (*E*)-α-bergamotene, indicating that this amino acid change does not affect the enzymatic function of the NaTPS38 protein (Fig. 6a). We then compared (*E*)-α-bergamotene emission among natural genotypes that carry different haplotypes. The genotypes that carry the YEI haplotype showed lower (*E*)-α-bergamotene emissions from both flowers and herbivory-induced leaves than those that harbor the YGI haplotype (Fig. 6b). Consistently, abundance of *NaTPS38* transcripts from the YEI haplotype carriers is also lower than those with the YGI haplotype (Fig. S3). Interestingly, the HGV haplotype showed intermediate (*E*)-α-bergamotene emission in both flowers and herbivory-induced leaves (Fig. 6b). While the floral transcript abundance of *NaTPS38* in HGV haplotype carriers is similar to that in YEI haplotype carriers, in terms of herbivory-induced leaf abundances, they are similar to YGI haplotype carriers (Fig. S3).

Because *NaTPS38* and *NaTPS25* are co-localized in the genome, we hypothesized that genetic variation of *NaTPS25* is also linked to the three different haplotypes of *NaTPS38*. Mapping *NaTPS25* presence/absence information in herbivory-induced leaves to the three haplotypes of *NaTPS38* showed that 80% (eight out of 10) of individuals that carried the *NaTPS38-YGI* haplotype also had no expression of *NaTPS25*, whereas individuals that carried the *NaTPS38-HGV* and *NaTPS38-YEI* haplotypes all had detectable *NaTPS25* transcript levels (Fig. 6a). Consistently, in both flowers and herbivory-induced leaves,

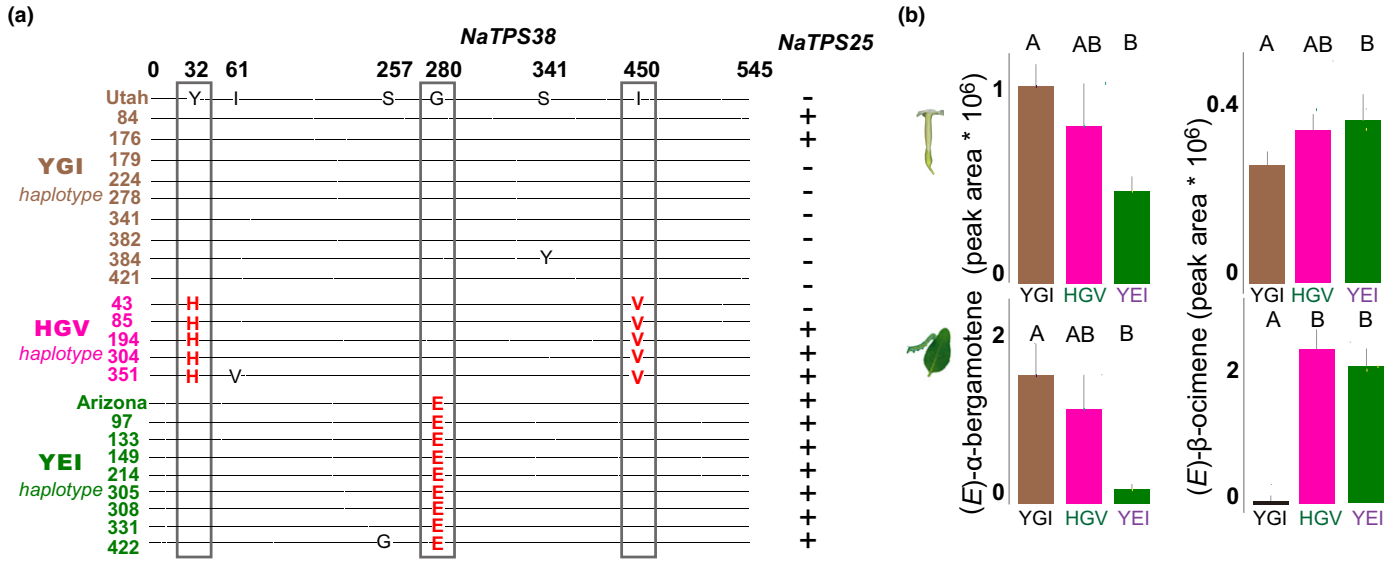


**Fig. 6** Allelic variations of the terpene cluster are associated with differences in floral volatiles and herbivory-induced plant volatiles (HIPVs) among *Nicotiana attenuata* natural accessions. (a) Three different haplotypes found from the open reading frame of *NaTPS38* from *N. attenuata* accessions. The amino acid sequence of *NaTPS38* from the Utah genotype is set as the reference, and the different haplotype loci are marked in red. The presence of an intact *NaTPS25* gene in the natural accessions is shown on the right (+, present; −, not present). (b) The emission of (*E*)-α-bergamotene and (*E*)-β-ocimene in both flowers and herbivory-induced leaves are different among three *NaTPS38* haplotypes. The data for (*E*)-α-bergamotene emission were extracted from our previous study (Zhou *et al*., 2017). Mean and SE are shown. Statistical differences among haplotypes were determined by ANOVA ($P < 0.05$).

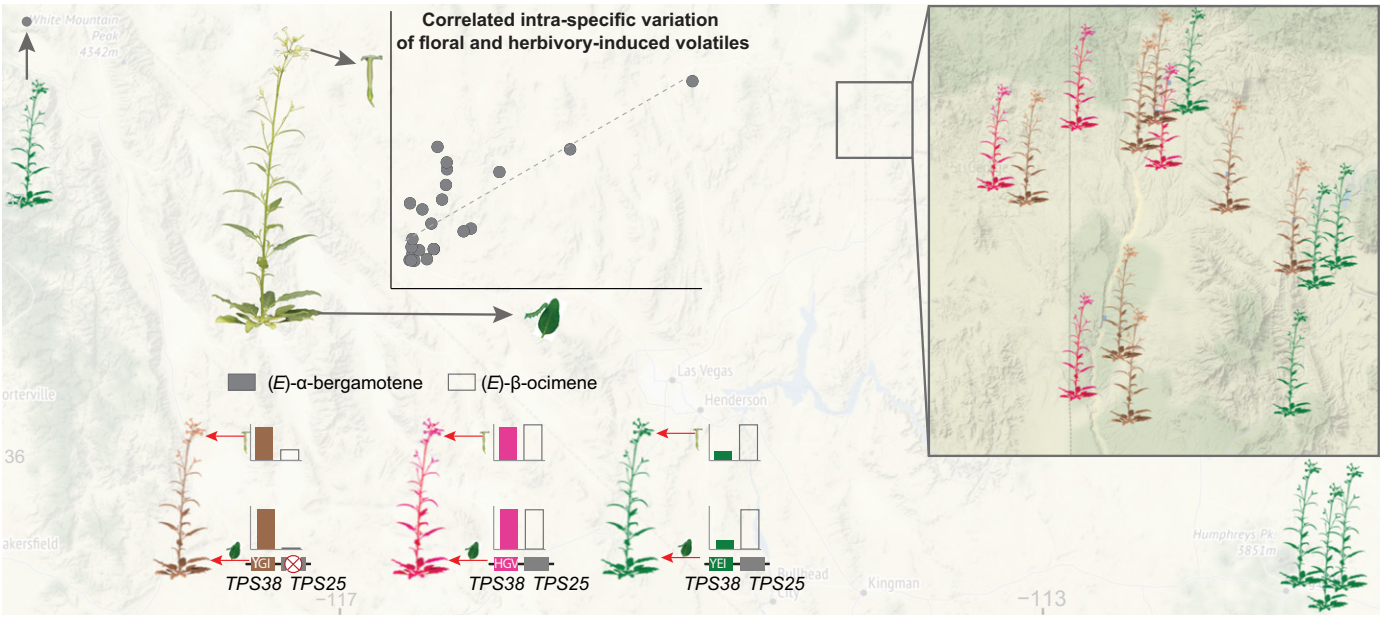


**Fig. 7** Summary model of allelic differences of the two linked terpene synthases contributing to correlated intraspecific variation of floral and herbivory-induced volatiles in *Nicotiana attenuata*. The locations of different genotypes are shown on the map. Color represents different *NaTPS38* haplotype groups: brown refers to YGI, pink refers to HGV and green refers to YEI.

individuals that carried the *NaTPS38-YGI* haplotype also accumulated only very low levels of *NaTPS25* transcripts and produced a lower amount of (*E*)-β-ocimene, whereas individuals that carried the *NaTPS38-YEI* haplotype accumulated high levels of *NaTPS25* transcripts and emitted high levels of (*E*)-β-ocimene (Figs 3a, 6b, S3c). Again, the *NaTPS38-HGV* haplotype plants showed intermediate *NaTPS25* transcript abundance but high levels of (*E*)-β-ocimene emission in both flowers and leaves (Figs 3a, 6b, S3c). These results reveal that the linked allelic differences of *NaTPS38* and *NaTPS25* in *N. attenuata* contributed to correlated changes in both floral volatiles and HIPVs (Fig. 7).

## Discussion

Intrinsic genetic linkage and pleiotropy have been proposed to explain correlated variation in floral and defense traits (Johnson

*et al.*, 2015). However, direct genetic evidence for this is scarce. Here, by exploring natural variation and using both forward and reverse genetics tools, we demonstrate that allelic differences in two clustered terpene synthase genes, *NaTPS25* and *NaTPS38*, result in correlated intraspecific variations of both HIPVs and floral volatiles in *N. attenuata*.

We found that variations in the emissions of two terpenoids, (*E*)-β-ocimene and (*E*)-α-bergamotene, showed correlated changes in HIPVs and floral volatile profiles (Fig. 1). (*E*)-β-ocimene is often found among HIPVs and floral headspace in different species (Farre-Armengol *et al.*, 2017). While (*E*)-β-ocimene in HIPVs can act as an important chemical cue for attracting natural enemies of phytophagous insects among plant species, it did not increase the attraction of predators of *M. sexta* larvae in *N. attenuata* in nature (Kessler & Baldwin, 2001). Floral (*E*)-β-ocimene emission is also common among flowering plants and can act as an attractant to generalist pollinators, such as bees and beetles (Farre-Armengol *et al.*, 2017). Although *N. attenuata* often attracts *M. sexta* as its pollinator, in some populations (e.g. Arizona), bees are also found to visit *N. attenuata* flowers (D. Kessler, personal communication). Therefore, it is plausible that floral (*E*)-β-ocimene emission in *N. attenuata* might increase bee-mediated pollination success. Different from (*E*)-β-ocimene, (*E*)-α-bergamotene emission has only been reported in a few species, such as maize and *N. attenuata*. In both maize and *N. attenuata*, (*E*)-α-bergamotene in HIPVs is important for indirect defense function (Kessler & Baldwin, 2001; Degen *et al.*, 2004). Although it remains unclear whether (*E*)-α-bergamotene is also emitted in floral tissues in maize, the present study showed that the flowers of *N. attenuata* emit (*E*)-α-bergamotene, which increases *M. sexta* moth-mediated pollination success (Zhou *et al.*, 2017). Therefore, the correlated changes of (*E*)-β-ocimene and (*E*)-α-bergamotene in HIPVs and floral volatiles can result in concerted adaptation to pollinators and herbivores in *N. attenuata*.

The changes of (*E*)-β-ocimene and (*E*)-α-bergamotene emissions in HIPVs and floral headspace are probably due to allelic variations of two clustered terpene synthase genes, *NaTPS25* and *NaTPS38*. This is supported by four independent lines of evidence. First, forward genetic mapping showed that the same locus is associated with the emissions of (*E*)-β-ocimene and (*E*)-α-bergamotene in HIPVs. Although it was difficult to find the responsible gene in the QTL directly from the fragmented *N. attenuata* genome assembly, synteny information between *N. attenuata* and tomato showed that the QTL probably contains a TPS cluster that includes *TPS25* and *TPS38*. Second, using reverse genetic approaches, we demonstrated that the expression of *NaTPS25* and *NaTPS38* were required for (*E*)-β-ocimene and (*E*)-α-bergamotene emission in HIPVs (Fig. 2; Zhou *et al.*, 2017), respectively. Among different natural accessions, the expression levels of *NaTPS25* and *NaTPS38* were furthermore correlated with (*E*)-β-ocimene and (*E*)-α-bergamotene emission, respectively, in both floral headspace and HIPVs (Fig. 2b; Zhou *et al.*, 2017). Third, *in vitro* enzymatic assays demonstrated the specific terpene synthase functions of both enzymes (Fig. 2; Zhou *et al.*, 2017). Fourth, allelic variation of *NaTPS38* and *NaTPS25* were tightly linked and formed three main haplotypes. Individuals carrying different haplotypes showed correlated changes in (*E*)-β-ocimene and (*E*)-α-bergamotene emissions in floral headspace and HIPVs (Fig 6).

While the correlated changes of (*E*)-α-bergamotene in HIPVs and floral volatiles are due to pleiotropy of *NaTPS38*, the correlated changes of (*E*)-β-ocimene in HIPVs and floral volatiles are probably due to genetic linkage. This is because some genotypes do not emit (*E*)-β-ocimene in HIPVs due to loss-of-function mutations in *NaTPS25*, but they still emit (*E*)-β-ocimene in flowers, although at relatively low levels. A plausible scenario is that a transcriptional regulator of another TPS that is involved in floral (*E*)-β-ocimene emissions is in strong genetic linkage with the *NaTPS25/38* locus. If this is the case, the correlation between emissions of (*E*)-β-ocimene in the floral headspace and in HIPVs might disappear when the genetic linkage is interrupted, for example among genotypes that harbor much more frequent recombination than we have analyzed or among closely related species.

We found two different genetic mechanisms are associated with allelic expression changes in *NaTPS25* and *NaTPS38*. While loss-of-function mutations mediated by a transposable element insertion resulted in expression variations of *NaTPS25*, changes at both *cis*- and *trans*-regulatory elements contributed to the different expression of *NaTPS38* among genotypes. The differences in underlying genetic mechanisms might be due to differences in fitness optima of (*E*)-α-bergamotene (one optimum peak, thus under stabilizing selection) and (*E*)-β-ocimene (two optimum peaks, thus under disruptive selection). However, it is currently unclear which stresses may favor loss-of-function in *NaTPS25*. Another explanation is that *NaTPS25* and *NaTPS38* have different pleiotropic functions. As silencing *NaTPS38* resulted in the complete absence of (*E*)-α-bergamotene in the HIPVs and floral volatile profiles (Zhou *et al.*, 2017), NaTPS38 is probably the only key enzyme that is responsible for the biosynthesis of (*E*)-α-bergamotene in both HIPVs and floral volatiles in *N. attenuata*. However, while silencing *NaTPS25* resulted in strong decreases in (*E*)-β-ocimene emission in HIPVs, genotypes (such as Utah) with loss-of-function in *NaTPS25* still emitted (*E*)-β-ocimene from flowers. This suggests that the biosynthesis of (*E*)-β-ocimene in flowers might be a result of several genes with similar functions in *N. attenuata*. Therefore, the level of functional pleiotropy for *NaTPS25* is lower than for *NaTPS38*. As a consequence, a loss-of-function mutation in *NaTP25* might be associated with less distinct fitness costs than for one in *NaTPS38*. This is consistent with the pattern observed from the genetic mechanisms underlying changes of floral color and scent (Hoballah *et al.*, 2007; Wessinger & Rausher, 2012; Xu *et al.*, 2012; Sas *et al.*, 2016; Sheehan *et al.*, 2016), in which loss-of-function mutations are more common than regulatory element changes in genes with less pleiotropy in their functions.

The intrinsic link between floral volatiles and HIPVs in natural populations of *N. attenuata* implies that intraspecific variation of plant volatiles can be maintained due to pleiotropy and/or genetic linkage. For example, when an *N. attenuata* population is under directional selection for high amounts of floral (*E*)-α-

bergamotene emission, either imposed by *M. sexta* moths or hummingbirds (both show strong preference for (*E*)-α-bergamotene (see Kessler & Baldwin, 2007)), individuals that carry the YGI haplotype would have higher fitness and the frequency of the YGI haplotype in the population would increase. As a consequence, the level of herbivory-induced (*E*)-α-bergamotene and (*E*)-β-ocimene emissions would increase in the population. In such a scenario, changes in HIPVs in these populations are not due to selection on HIPVs, but rather are due to the pleiotropy or genetic linkage of the YGI haplotype, which is also associated with high levels of herbivory-induced (*E*)-α-bergamotene and low levels of (*E*)-β-ocimene emission. The same logic may also apply to how selection on HIPVs could result in changes in floral volatiles.

The presence of genetic linkage and pleiotropy between HIPVs and floral volatiles suggest that plant volatiles might evolve under diffuse selection imposed from herbivores and pollinators in *N. attenuata* (Iwao & Rausher, 1997; Strauss & Irwin, 2004; Agrawal & Stinchcombe, 2009; Wise & Rausher, 2013). Diffuse coevolution can be common for plant resistance to multiple-herbivore communities (Wise & Rausher, 2013) and recent genetic analyses have discovered correlated changes of chemical defense compounds among tissues (Chan *et al.*, 2011; Keith & Mitchell-Olds, 2019) which were due to genetic linkage or pleiotropy, similar to the two terpenoids we found here. It is plausible that many other metabolic traits also show correlated changes among tissues, although future studies using comparative metabolomics and transcriptomics approaches are needed to further examine this. Diffuse interactions with multiple-herbivore communities and correlated changes of chemical defenses among tissues often constrain the evolution of plant resistance (Wise & Rausher, 2013; Keith & Mitchell-Olds, 2019). Because plant–herbivore and plant–pollinator interactions are often studied in isolation (Lucas-Barbosa, 2016), the extent to which diffuse interactions exist within plant–herbivore and plant–pollinator interactions, and their evolutionary consequences, remain largely unclear. One recent study using an experimental evolution approach has demonstrated a diffuse coevolution of floral signals and plant direct defenses in *Brassica rapa* (Ramos & Schiestl, 2019), although this study did not investigate genetic correlation of floral signals and plant defenses. The studies and results reported here highlight the importance of investigating trait evolution in a community context (Strauss & Irwin, 2004). Prospective studies deploying experimental evolution approaches, in which the multigenerational fitness of different genotypes is determined under manipulated selection agents in their native habitat, will be needed to provide complementary understanding on how adaptive traits evolve in nature.

## Acknowledgements

We thank Dr M. Huber and Dr M. Schäfer for critical comments on an earlier version of the manuscript, and three reviewers for constructive suggestions. We are grateful to the help from Anke Kügler for sample collections. This work was supported by funding from the Swiss National Science Foundation (PEBZP3-142886 to SX), a European Commission Marie Curie Intra-European Fellowship (IEF, 328935 to SX), the Max Planck Society, and a European Research Council Advanced Grant (ClockworkGreen 293926 to ITB).

## Author contributions

Conceptualization, SX; methodology, WZ, SX, CK, EM, NDL, HG, TGK, ITB and MCS; investigation, WZ, SX, CK, EM, NDL, HG, TGK and MCS; writing, SX, WZ; review and editing, SX, WZ, CK, EM, NDL, HG, TGK, MCS and ITB; funding acquisition, SX, ITB; resources, SX and ITB.

## ORCID

Ian T. Baldwin https://orcid.org/0000-0001-5371-2974
Han Guo https://orcid.org/0000-0001-9118-9897
Tobias G. Köllner https://orcid.org/0000-0002-7037-904X
Erica McGale https://orcid.org/0000-0002-5996-4213
Meredith C. Schuman https://orcid.org/0000-0003-3159-3534
Shuqing Xu https://orcid.org/0000-0001-7010-4604
Wenwu Zhou https://orcid.org/0000-0002-0727-8086

## References

**Agrawal AF, Stinchcombe JR. 2009.** How much do genetic covariances alter the rate of adaptation? *Proceedings of the Royal Society B: Biological Sciences* **276**: 1183–1191.

**Allmann S, Baldwin IT. 2010.** Insects betray themselves in nature to predators by rapid isomerization of green leaf volatiles. *Science* **329**: 1075–1078.

**Baldwin IT. 2010.** Plant volatiles. *Current Biology* **20**: R392–R397.

**Boutanaev AM, Moses T, Zi JC, Nelson DR, Mugford ST, Peters RJ, Osbourn A. 2015.** Investigation of terpene diversification across multiple sequenced plant genomes. *Proceedings of the National Academy of Sciences, USA* **112**: E81–E88.

**Brockmöller T, Ling Z, Li D, Gaquerel E, Baldwin IT, Xu S. 2017.** *Nicotiana attenuata* Data Hub (NaDH): an integrative platform for exploring genomic, transcriptomic and metabolomic data in wild tobacco. *BMC Genomics* **18**: 79.

**Bubner B, Gase K, Baldwin IT. 2004.** Two-fold differences are the detection limit for determining transgene copy numbers in plants by real-time PCR. *BMC Biotechnology* **4**: 14.

**Chan EKF, Rowe HC, Corwin JA, Joseph B, Kliebenstein DJ. 2011.** Combining genome-wide association mapping and transcriptional networks to identify novel genes controlling glucosinolates in *Arabidopsis thaliana*. *PLoS Biology* **9**: 8.

**Chen H, Köllner TG, Li G, Wei G, Chen X, Zeng D, Qian Q, Chen F. 2020.** Combinatorial evolution of a terpene synthase gene cluster explains terpene variations in *Oryza*. *Plant Physiology* **182**: 480–492.

**Chen X, Luck K, Rabe P, Dinh CQD, Shaulsky G, Nelson DR, Gershenzon J, Dickschat JS, Köllner TG, Chen F. 2019.** A terpene synthase-cytochrome P450 cluster in *Dictyostelium discoideum* produces a novel trisnorsesquiterpene. *eLife* **8**: e44352.

**Cheng R, Abney M, Palmer AA, Skol AD. 2011.** QTLRel: an R package for genome-wide association studies in which relatedness is a concern. *BMC Genetics* **12**: 66.

**Degen T, Dillmann C, Marion-Poll F, Turlings TCJ. 2004.** High genetic variability of herbivore-induced volatile emission within a broad range of maize inbred lines. *Plant Physiology* **135**: 1928–1938.

**Degenhardt J, Hiltpold I, Köllner TG, Frey M, Gierl A, Gershenzon J, Hibbard BE, Ellersieck MR, Turlings TCJ. 2009.** Restoring a maize root signal that

attracts insect-killing nematodes to control a major pest. *Proceedings of the National Academy of Sciences, USA* **106**: 13213–13218.

**Dicke M. 1994.** Local and systemic production of volatile herbivore-induced terpenoids – their role in plant–carnivore mutualism. *Journal of Plant Physiology* **143**: 465–472.

**Falara V, Akhtar TA, Nguyen TTH, Spyropoulou EA, Bleeker PM, Schauvinhold I, Matsuba Y, Bonini ME, Schilmiller AL, Last RL *et al.* 2011.** The tomato terpene synthase gene family. *Plant Physiology* **157**: 770–789.

**Farre-Armengol G, Filella I, Llusia J, Penuelas J. 2017.** β-Ocimene, a key floral and foliar volatile involved in multiple interactions between plants and other organisms. *Molecules* **22**: 1148.

**Fraser AM, Mechaber WL, Hildebrand JG. 2003.** Electroantennographic and behavioral responses of the sphinx moth *Manduca sexta* to host plant headspace volatiles. *Journal of Chemical Ecology* **29**: 1813–1833.

**Galis I, Schuman MC, Gase K, Hettenhausen C, Hartl M, Dinh ST, Wu J, Bonaventure G, Baldwin IT. 2013.** The use of VIGS technology to study plant–herbivore interactions. In: Becker A, ed. *Virus-induced gene silencing*. Totowa, NJ, USA: Humana Press, 109–137.

**Gaquerel E, Weinhold A, Baldwin IT. 2009.** Molecular interactions between the specialist herbivore *Manduca sexta* (Lepidoptera, Sphigidae) and its natural host *Nicotiana attenuata*. VIII. An unbiased GCxGC-ToFMS analysis of the plant's elicited volatile emissions. *Plant Physiology* **149**: 1408–1423.

**Grabherr MG, Haas BJ, Yassour M, Levin JZ, Thompson DA, Amit I, Adiconis X, Fan L, Raychowdhury R, Zeng QD *et al.* 2011.** Full-length transcriptome assembly from RNA-seq data without a reference genome. *Nature Biotechnology* **29**: 644–652.

**Guo H, Halitschke R, Wielsch N, Gase K, Baldwin IT. 2019.** Mate selection in self-compatible wild tobacco results from coordinated variation in homologous self-incompatibility genes. *Current Biology* **29**: 2020–2030.

**Guo H, Lackus ND, Köllner TG, Li R, Bing J, Wang Y, Baldwin IT, Xu S. 2020.** Evolution of a novel and adaptive floral scent in wild tobacco. *Molecular Biology and Evolution* **37**: 1090–1099.

**Halitschke R, Kessler A, Kahl J, Lorenz A, Baldwin IT. 2000.** Ecophysiological comparison of direct and indirect defenses in *Nicotiana attenuata*. *Oecologia* **124**: 408–417.

**Halitschke R, Stenberg JA, Kessler D, Kessler A, Baldwin IT. 2008.** Shared signals – 'alarm calls' from plants increase apparency to herbivores and their enemies in nature. *Ecology Letters* **11**: 24–34.

**He J, Fandino RA, Halitschke R, Luck K, Kollner TG, Murdock MH, Ray R, Gase K, Knaden M, Baldwin IT *et al.* 2019.** An unbiased approach elucidates variation in (*S*)-(+)-linalool, a context-specific mediator of a tri-trophic interaction in wild tobacco. *Proceedings of the National Academy of Sciences, USA* **116**: 14651–14660.

**Hoballah ME, Gubitz T, Stuurman J, Broger L, Barone M, Mandel T, Dell'Olivo A, Arnold M, Kuhlemeier C. 2007.** Single gene-mediated shift in pollinator attraction in *Petunia*. *Plant Cell* **19**: 779–790.

**Huang MS, Abel C, Sohrabi R, Petri J, Haupt I, Cosimano J, Gershenzon J, Tholl D. 2010.** Variation of herbivore-induced volatile terpenes among Arabidopsis ecotypes depends on allelic differences and subcellular targeting of two terpene synthases, TPS02 and TPS03. *Plant Physiology* **153**: 1293–1310.

**Irmisch S, Krause ST, Kunert G, Gershenzon J, Degenhardt J, Köllner TG. 2012.** The organ-specific expression of terpene synthase genes contributes to the terpene hydrocarbon composition of chamomile essential oils. *BMC Plant Biology* **12**: 84.

**Iwao K, Rausher MD. 1997.** Evolution of plant resistance to multiple herbivores: quantifying diffuse coevolution. *The American Naturalist* **149**: 316–335.

**Johnson MTJ, Campbell SA, Barrett SCH. 2015.** Evolutionary interactions between plant reproduction and defense against herbivores. *Annual Review of Ecology, Evolution, and Systematics* **46**: 191–213.

**Kallenbach M, Oh Y, Eilers EJ, Veit D, Baldwin IT, Schuman MC. 2014.** A robust, simple, high-throughput technique for time-resolved plant volatile analysis in field experiments. *The Plant Journal* **78**: 1060–1072.

**Keith RA, Mitchell-Olds T. 2019.** Antagonistic selection and pleiotropy constrain the evolution of plant chemical defenses. *Evolution* **73**: 947–960.

**Kessler A, Baldwin IT. 2001.** Defensive function of herbivore-induced plant volatile emissions in nature. *Science* **291**: 2141–2144.

**Kessler D, Baldwin IT. 2007.** Making sense of nectar scents: the effects of nectar secondary metabolites on floral visitors of *Nicotiana attenuata*. *The Plant Journal* **49**: 840–854.

**Kessler D, Gase K, Baldwin IT. 2008.** Field experiments with transformed plants reveal the sense of floral scents. *Science* **321**: 1200–1202.

**Krügel T, Lim M, Gase K, Halitschke R, Baldwin IT. 2002.** Agrobacterium-mediated transformation of *Nicotiana attenuata*, a model ecological expression system. *Chemoecology* **12**: 177–183.

**Lee S, Badieyan S, Bevan DR, Herde M, Gatz C, Tholl D. 2010.** Herbivore-induced and floral homoterpene volatiles are biosynthesized by a single P450 enzyme (CYP82G1) in Arabidopsis. *Proceedings of the National Academy of Sciences, USA* **107**: 21205–21210.

**Lucas-Barbosa D. 2016.** Integrating studies on plant–pollinator and plant–herbivore interactions. *Trends in Plant Science* **21**: 125–133.

**Martin DM, Aubourg S, Schouwey MB, Daviet L, Schalk M, Toub O, Lund ST, Bohlmann J. 2010.** Functional annotation, genome organization and phylogeny of the grapevine (*Vitis vinifera*) terpene synthase gene family based on genome assembly, FLcDNA cloning, and enzyme assays. *BMC Plant Biology* **10**: 226.

**Matsuba Y, Nguyen TTH, Wiegert K, Falara V, Gonzales-Vigil E, Leong B, Schafer P, Kudrna D, Wing RA, Bolger AM *et al.* 2013.** Evolution of a complex locus for terpene biosynthesis in *Solanum*. *Plant Cell* **25**: 2022–2036.

**Nagegowda DA. 2010.** Plant volatile terpenoid metabolism: biosynthetic genes, transcriptional regulation and subcellular compartmentation. *FEBS Letters* **584**: 2965–2973.

**Oh Y, Baldwin IT, Galis I. 2013.** A jasmonate ZIM-domain protein NaJAZd regulates floral jasmonic acid levels and counteracts flower abscission in *Nicotiana attenuata* plants. *PLoS ONE* **8**: e57868.

**R Core Team. 2016.** *R: a language and environment for statistical computing*. [WWW document] URL https://www.R-project.org/ [accessed 1 December 2016].

**Raguso RA. 2008.** Wake up and smell the roses: the ecology and evolution of floral scent. *Annual Review of Ecology, Evolution, and Systematics* **39**: 549–569.

**Raguso RA. 2016.** More lessons from linalool: insights gained from a ubiquitous floral volatile. *Current Opinion in Plant Biology* **32**: 31–36.

**Ramos SE, Schiestl FP. 2019.** Rapid plant evolution driven by the interaction of pollination and herbivory. *Science* **364**: 193–196.

**Sas C, Muller F, Kappel C, Kent TV, Wright SI, Hilker M, Lenhard M. 2016.** Repeated inactivation of the first committed enzyme underlies the loss of benzaldehyde emission after the selfing transition in *Capsella*. *Current Biology* **26**: 3313–3319.

**Schuman MC, Allmann S, Baldwin IT. 2015.** Plant defense phenotypes determine the consequences of volatile emission for individuals and neighbors. *eLife* **4**: e04490.

**Schuman MC, Barthel K, Baldwin IT. 2012.** Herbivory-induced volatiles function as defenses increasing fitness of the native plant *Nicotiana attenuata* in nature. *eLife* **1**: e00007.

**Schuman MC, Heinzel N, Gaquerel E, Svatos A, Baldwin IT. 2009.** Polymorphism in jasmonate signaling partially accounts for the variety of volatiles produced by *Nicotiana attenuata* plants in a native population. *New Phytologist* **183**: 1134–1148.

**Schuman MC, Palmer-Young EPC, Schmidt A, Gershenzon J, Baldwin IT. 2014.** Ectopic TPS expression enhances sesquiterpene emission in *Nicotiana attenuata* without altering defense or development of transgenic plants or neighbors. *Plant Physiology* **166**: 779–797.

**Sheehan H, Moser M, Klahre U, Esfeld K, Dell'Olivo A, Mandel T, Metzger S, Vandenbussche M, Freitas L, Kuhlemeier C. 2016.** MYB-FL controls gain and loss of floral UV absorbance, a key trait affecting pollinator preference and reproductive isolation. *Nature Genetics* **48**: 159–166.

**Sime KR, Baldwin IT. 2003.** Opportunistic out-crossing in *Nicotiana attenuata* (Solanaceae), a predominantly self-fertilizing native tobacco. *BMC Ecology* **3**: 6.

**Steppuhn A, Schuman MC, Baldwin IT. 2008.** Silencing jasmonate signalling and jasmonate-mediated defences reveals different survival strategies between two *Nicotiana attenuata* accessions. *Molecular Ecology* **17**: 3717–3732.

**Strauss SY, Irwin RE. 2004.** Ecological and evolutionary consequences of multispecies plant–animal interactions. *Annual Review of Ecology Evolution and Systematics* **35**: 435–466.

**Tholl D. 2006.** Terpene synthases and the regulation, diversity and biological roles of terpene metabolism. *Current Opinion in Plant Biology* **9**: 297–304.

**Turlings TC, Wäckers F. 2004.** Recruitment of predators and parasitoids by herbivore-injured plants. *Advances in Insect Chemical Ecology* **2**: 21–75.

**van Schie CCN, Haring MA, Schuurink RC. 2006.** Regulation of terpenoid and benzenoid production in flowers. *Current Opinion in Plant Biology* **9**: 203–208.

**Wessinger CA, Rausher MD. 2012.** Lessons from flower colour evolution on targets of selection. *Journal of Experimental Botany* **63**: 5741–5749.

**Wise MJ, Rausher MD. 2013.** Evolution of resistance to a multiple-herbivore community: genetic correlations, diffuse coevolution, and constraints on the plant's response to selection. *Evolution* **67**: 1767–1779.

**Wittkopp PJ. 2013.** Evolution of gene expression. In: Losos JB, ed. *The Princeton guide to evolution*. Princeton, NJ, USA: Princeton University Press, 413–419.

**Wu JQ, Hettenhausen C, Schuman MC, Baldwin IT. 2008.** A comparison of two *Nicotiana attenuata* accessions reveals large differences in signaling induced by oral secretions of the specialist herbivore *Manduca sexta*. *Plant Physiology* **146**: 927–939.

**Xu S, Schlüter PM, Grossniklaus U, Schiestl FP. 2012.** The genetic basis of pollinator adaptation in a sexually deceptive orchid. *PLoS Genetics* **8**: e1002889.

**Zhou WW, Kuegler A, McGale E, Haverkamp A, Knaden M, Guo H, Beran F, Yon F, Li R, Lackus N *et al.* 2017.** Tissue-specific emission of (*E*)-alpha-bergamotene helps resolve the dilemma when pollinators are also herbivores. *Current Biology* **27**: 1336–1341.

## Supporting Information

Additional Supporting Information may be found online in the Supporting Information section at the end of the article.

**Fig. S1** Differences in the putative promoter region of *NaTPS38* between the Arizona and Utah genotypes.

**Fig. S2** Protein structure model of NaTPS38.

**Fig. S3** Transcript abundance of *NaTPS38* and *NaTPS25* alleles among different NaTPS38 haplotypes in *Nicotiana attenuata*.

**Table S1** GPS coordinates of the location where the 25 *Nicotiana attenuata* natural accessions were originally collected.

**Table S2** The primer sets used in this study.

Please note: Wiley-Blackwell are not responsible for the content or functionality of any supporting information supplied by the authors. Any queries (other than missing material) should be directed to the *New Phytologist* Central Office.